

# Ethanol extract of *Patrinia scabiosaefolia* induces the death of human renal cell carcinoma 786-O cells via SIRT-1 and mTOR signaling-mediated metabolic disruptions

ZHEYAN LI<sup>1\*</sup>, YUEQING TANG<sup>1\*</sup>, SHIQIN ZHU<sup>2</sup>, DAWEI LI<sup>1</sup>, XIAO HAN<sup>1</sup>, GANGLI GU<sup>1</sup>, NAIDONG XING<sup>1</sup>, JUCHAO REN<sup>1</sup>, ZHAOXIN GUO<sup>1</sup>, WEI JIAO<sup>1</sup>, LEI YAN<sup>1</sup>, ZHONGHUA XU<sup>1</sup> and WENHUA ZHANG<sup>1</sup>

<sup>1</sup>Department of Urology, Qilu Hospital of Shandong University; <sup>2</sup>Department of Biochemistry, Shandong University, Jinan, Shandong 250012, P.R. China

Received April 16, 2017; Accepted October 17, 2017

DOI: 10.3892/or.2017.6139

**Abstract.** Recently, natural plant extracts have shown tremendous potential as novel antitumor drugs. *Patrinia scabiosaefolia*, a traditional prescription for inflammatory diseases, has been reported to effectively suppress various types of cancers. However, the mechanisms underlying its antitumor properties remain elusive. In the present study, we investigated the antitumor effects of an ethanol extract of *Patrinia scabiosaefolia* (EPS) on human renal cell carcinoma 786-O cells. After 24 h of incubation with EPS, the cell viability and colony number of 786-O cells were significantly decreased in a concentration-dependent manner as compared to the control group as determined by MTT and colony formation assays, respectively. The necrotic rate and apoptotic rate in the EPS exposure group were significantly higher than these rates noted in the control group as revealed by LDH release assay and Hoechst 33342/PI double staining, respectively. At the concentration of 1.0 mg/ml, the necrotic and apoptotic rates reached 41.7±6.6 and 7.8±1.4%, respectively (P<0.01). However, the fluorescence intensity of intracellular calcium concentration ( $[Ca^{2+}]_i$ ) was markedly elevated from 0.029±0.0007 to 0.060±0.003 (P<0.001) after the intervention of EPS. Moreover, the fluorescence intensity of intracellular ROS in the EPS exposure group was significantly higher

(0.074±0.005) compared to that observed in the control group (0.033±0.001, P<0.001), which was partly attenuated by the specific antioxidant *N*-acetylcysteine (NAC). Furthermore, our results demonstrated that EPS significantly downregulated the expression of SIRT-1 and obviously induced the dephosphorylation of mTOR. Moreover, combined treatment with the SIRT-1 inhibitor nicotinamide and EPS was able to significantly enhance the induction of necrosis and reduction in cell viability of 786-O cells noted following treatment with EPS alone. In summary, we conclude that EPS induced the death of 786-O cells via SIRT-1 and mTOR signaling-mediated metabolic disruptions, which provide novel insight into the application of natural plant extracts for the treatment of cancers.

## Introduction

Traditional Chinese medicine (TCM), including various natural plant extracts, has shown tremendous potential for the discovery of alternative drugs for the treatment of cancer (1,2). Fewer adverse effects and cost effectiveness endow TCM great advantages over Western chemotherapeutics (3). *Patrinia scabiosaefolia*, a perennial plant mainly distributed in East Asia, is extensively prescribed for various diseases, such as oxidative damage (4), inflammation (5), tumors (6) and edema (7). Of all the above-mentioned effects, antitumor activity is a prominent characteristic of *Patrinia scabiosaefolia*. Peng *et al* reported the *Patrinia scabiosaefolia* inhibited the growth of different cancer cell models including colorectal cancer mouse tumor tissues, HT-29 and U266 through G1/S cell cycle arrest, suppression of tumor angiogenesis and the STAT3 pathway, respectively (6,8,9). A previous study demonstrated that *Patrinia scabiosaefolia* induced the apoptosis of breast carcinoma MCF-7 cells without caspase-9 activation (10). However, the mechanisms underlying its antitumor properties remain elusive, and the antitumor effects of *Patrinia scabiosaefolia* deserve increased attention.

Recently, research which has focused on exploiting metabolic perturbations in the area of cancer therapy has been extensively investigated (11). ROS homeostasis serves as a critical factor for the survival of cancer cells. There is

---

Correspondence to: Dr Zhonghua Xu or Dr Wenhua Zhang, Department of Urology, Qilu Hospital of Shandong University, Wenhua Road 44, Jinan, Shandong 250012, P.R. China  
E-mail: xuzhonghua1963@163.com  
E-mail: summerdays123@126.com

\*Contributed equally

**Abbreviations:** EPS, ethanol extract of *Patrinia scabiosaefolia*; ROS, reactive oxygen species; SIRT-1, sirtuin-1; mTOR, mammalian target of rapamycin

**Key words:** *Patrinia scabiosaefolia*, 786-O cells, antitumor, metabolic disruptions, SIRT-1, mTOR

evidence indicating that cancer cells are more vulnerable to high levels of ROS (12), which further evokes a series of metabolic dysfunction, such as apoptosis, calcium overload and bio-macromolecule degradation (13-15). The calcium ion, as a ubiquitous secondary messenger, induces intracellular ROS generation. In turn, ROS can regulate the  $Ca^{2+}$  signaling pathway (14). Excessive accumulation of ROS and calcium overload can initiate the apoptotic pathway (16). The reciprocal interactions of the above three alterations intensively promote the death processes of cancer cells. Thus, manipulation of metabolic disruptions of cancer cells may be a promising target for cancer treatment.

SIRT-1, as an  $NAD^+$ -dependent deacetylase, has been demonstrated to regulate extensive cellular metabolic processes including cell stress response, apoptosis and lifespan extension (17-19). A previous study indicated that excessive expression of SIRT-1 in large B-cell lymphoma was closely related to poor patient prognosis (20). Recently, SIRT-1 has been demonstrated to function as an oncoprotein and tumor promoter in various types of cancer cells (21,22). Mammalian target of rapamycin (mTOR), a serine/threonine protein kinase, has been widely accepted to regulate cell growth and proliferation (23). Various chronic diseases, such as cancer, ageing and diabetes, are closely correlated with mTOR (24). There is evidence indicating that mTOR-dependent mechanisms are responsible for the tumorigenesis of many types of cancers (25). Thus, we speculated that SIRT-1 and mTOR may be involved in the EPS-induced antitumor effects.

In the present study, we investigated the antitumor effects of an ethanol extract of *Patrinia scabiosaeifolia* (EPS) on 786-O cells. MTT assay, colony formation assay and Hoechst/propidium iodide (PI) staining were performed to detect the inhibition of proliferation and the pro-apoptotic effects of EPS. Intracellular ROS and  $Ca^{2+}$  were examined to identify the metabolic disruptions induced by EPS. However, we conducted western blotting to explore the expression of SIRT-1 and mTOR after EPS stimulation. Furthermore, the above antitumor effects were found to be augmented by the SIRT-1 inhibitor nicotinamide. Thus, we conclude that EPS induced the death of 786-O cells via SIRT-1 and mTOR signaling-mediated metabolic disruptions.

## Materials and methods

**Cell culture and reagents.** Human renal cell carcinoma 786-O cells were cultured in RPMI-1640 medium supplemented with 10% fetal bovine serum (FBS), and human proximal tubular cells (HK-2) were cultured in Dulbecco's modified Eagle's medium (DMEM)/F12 (1:1) supplemented with 10% FBS (all from HyClone, Logan, UT, USA). Both types of cells were cultured under the condition of 95% humidity and 5%  $CO_2$  at 37°C. After passaging, the cells were cultured for 24 h and then treated with different concentrations of EPS for 24 h. MTT was provided by Solarbio (Beijing, China). Hoechst 33342 and PI, reactive oxygen species assay kit, Fluo-3 AM probe, *N*-acetylcysteine (NAC) and LDH cytotoxicity assay kit were purchased from Beyotime Biotechnology (Shanghai, China). Antibodies for SIRT-1, p-mTOR, mTOR and GAPDH were purchased from Cell Signaling Technology (Danvers, MA, USA). All other reagents used were commercially available.

**Preparation of an ethanol extract of *Patrinia scabiosaeifolia*.** *Patrinia scabiosaeifolia* Link (also named *Patrinia hispida* Bunge and *Patrinia scabiosaeifolia* Fisch. ex Trev (Caprifoliaceae family) was provided by Shennong Bencao Pharmacy (Shandong, China) and authenticated by Professor Aidong Lang, the analyst of the School of Pharmacy at Shandong University. Dry herbs of *Patrinia scabiosaeifolia* (the plant name has already been verified with <http://www.theplantlist.org>) of 1 kg were drenched in 95% ethanol (10 l) for 3 days, and then filtered. The filtrates were evaporated in a vacuum evaporator. The relative density was determined as 1.05. The EPS powder was obtained by a freeze-dryer. Subsequently, EPS was dissolved in dimethyl sulfoxide (DMSO) to produce a stock solution with the concentration of 300 mg/ml. The final concentrations of DMSO in all the culture medium were <0.5%. *Patrinia scabiosaeifolia* specimen was deposited at the Urology Laboratory of Cardiovascular Research Center in Qilu Hospital of Shandong University.

**MTT assay.** MTT assay was performed to evaluate the cell viability of 786-O and HK-2 cells. 786-O and HK-2 cells were seeded into 96-well plates at a density of  $5 \times 10^3$ /well, and incubated with different concentrations of EPS for 24 h. Subsequently, MTT (0.5 mg/ml) was added into each well and the cells were incubated for 4 h under conditions of 37°C and 5%  $CO_2$ . Then, the supernatant was removed and the formazan crystals were dissolved in 100  $\mu$ l DMSO. The absorption value was measured at 570 nm by an ELISA reader (Thermo Multiskan MK3; Thermo Fisher Scientific, Waltham, MA, USA).

**Colony formation assay.** 786-O cells were seeded in 6-well plates at the density of  $1 \times 10^3$ /well, and were then cultured for 10-14 days after stimulations. When colonies were visible, the incubation was terminated. Subsequently, the cells were rinsed with phosphate-buffered saline (PBS) and stained with crystal violet after being fixed with methanol. Colonies >50 cells were counted under a microscope with low magnification.

**Hoechst 33342 and PI double staining.** Hoechst/PI double staining was conducted to examine the apoptotic rate of 786-O cells. In brief, 786-O cells were cultured with 10  $\mu$ g/ml Hoechst 33342 and PI at 37°C for 15 min and then rinsed with PBS three times after stimulation. Morphological alterations of 786-O cells were observed by fluorescence microscope (Carl Zeiss SAS, Jena, Germany). Hoechst 33342 can penetrate the normal cell membrane, whereas PI merely penetrates the damaged cell membrane. Cell staining with Hoechst 33342 manifests blue fluorescence, whereas cells stained with PI manifest red fluorescence. The apoptotic rate and necrotic rate of 786-O cells were identified as the percentages of apoptotic cell nuclei and necrotic cell nuclei in five random fields.

**LDH release assay.** To further verify the necrosis promoting effect of EPS, LDH release assay was conducted. 786-O cells were plated in a 96-well at the density of  $5 \times 10^3$ /well. After a 24-h treatment with EPS, 100  $\mu$ l of the supernatant was transferred to a clear 96-well plate, and then 50  $\mu$ l LDH reaction working solution was added to each well for 30 min at room temperature. Subsequently, the absorption value was measured

at 490 nm by an ELISA reader (Thermo Multiskan MK3). The relative LDH activity was represented by the following equation:  $(OD_{\text{sample}} - OD_{\text{blank}})/(OD_{\text{max}} - OD_{\text{blank}})$ .

**ROS assay.** ROS assay was performed to investigate the level of intracellular ROS. 786-O cells were seeded into a 24-well at the density of  $3 \times 10^4$ /well. The cells were co-incubated with 250  $\mu$ l DCFH-DA probe (10  $\mu$ M, 1:1,000 diluted with RPMI-1640 medium) at 37°C for 20 min after stimulation. Then, the cells were rinsed with medium for three times and 200  $\mu$ l of the medium was added into every well. All the images were captured by fluorescence microscopy and the fluorescent intensity was analyzed by ImageJ software [National Institutes of Health (NIH), Bethesda, MD, USA].

**$[Ca^{2+}]_i$  measurement.** 786-O cells were plated into a 24-well plate at the density of  $3 \times 10^4$ /well. After EPS stimulation, the cells were washed by PBS, and then incubated with 5  $\mu$ M Fluo-3 AM probe for 30 min at 37°C. Subsequently, the cells were washed with PBS and then observed by fluorescence microscopy. The fluorescence intensity analysis was performed by ImageJ software.

**Western blotting.** 786-O cells were harvested by RIPA buffer plus phenylmethylsulfonyl fluoride (PMSF), and then total proteins were collected after stimulation. The concentrations of proteins were measured using the BCA method. Protein samples were subjected to 10% sodium dodecyl sulfate-polyacrylamide gel electrophoresis (SDS-PAGE). The protein bands of interest were subsequently electrotransferred to a nitrocellulose (NC) membrane and blocked with 5% skim milk for 1 h at room temperature. Incubations were conducted with primary antibodies (1:1,000) against GAPDH, p-mTOR, mTOR and SIRT-1 at 4°C overnight and subsequently secondary antibodies (1:5000) under room temperature for 1 h. After that, the gray scale values of the bands were detected using western immunoblotting detection (ECL system) reagents and then semi-quantitative analyzed by ImageJ software.

**Statistical analysis.** All data are presented as mean  $\pm$  standard error of the mean (SEM). Statistical analyses were conducted with one-way analysis of variance (ANOVA) followed by Tukey's post hoc analysis and unpaired t-test. The value of  $P < 0.05$  was considered as statistically significant. In addition, GraphPad Prism software (GraphPad Software, Inc., La Jolla, CA, USA) was used in all processes of the statistical analysis.

## Results

**EPS significantly inhibits the proliferation and growth of 786-O and HK-2 cells.** The ethanol extract of *Patrinia scabiosaefolia* (EPS) exhibited significant antiproliferation effects on the 786-O cells. Under the stimulation of EPS, cell viability of the cells was markedly decreased in both concentration-dependent and time-dependent manners compared to the control group. At the concentration of 0.6 mg/ml, 786-O cells exposed to EPS had a cell viability of  $0.49 \pm 0.12$  ( $P < 0.05$ ), whereas, there was only  $0.14 \pm 0.01$  ( $P < 0.001$ ) viability when the concentration reached 1.0 mg/ml (Fig. 1B). Morphological alterations were consistent with

the above results. The cells shrunk into a bright-round shape and less number of cells were noted with shorter processes following treatment with EPS. These damages were enhanced with the increasing EPS concentration (Fig. 1A). The time-dependent manner of the antiproliferation effects was also determined by MTT assay (Fig. 1C). Furthermore, as shown in Fig. 1D and E, the colony count significantly decreased from  $100.0 \pm 1.5$  to  $20.3 \pm 0.9$  when the cells were co-incubated with EPS at 0.2 mg/ml for 24 h ( $P < 0.001$ ). Whereas, almost no colonies could be observed under the concentration of 0.6 mg/ml EPS ( $P < 0.001$ ).

Human proximal tubular cells (HK-2) were also used to investigate the effects of EPS on normal cells. As shown in Fig. 1D, the cell viability of the HK-2 cells was significantly decreased in a concentration-dependent manner. Cell viabilities of  $0.793 \pm 0.062$  ( $P < 0.001$ ) and  $0.257 \pm 0.013$  ( $P < 0.001$ ), respectively were noted at concentrations of 0.6 and 1.0 mg/ml.

**EPS significantly promotes apoptosis and necrosis of 786-O cells.** Apoptosis, which is characterized by chromatin condensation and nuclear shrinkage, is identified by bright blue fluorescence following staining with Hoechst 33342/PI. In contrast, red fluorescence indicates necrotic cells due to the penetration of PI and viable cells show dull blue fluorescence. As shown in Fig. 2, more necrotic and apoptotic cells were detected in the EPS stimulation group as compared to the control group. At the concentration of 0.6 mg/ml, the apoptotic rate was  $8.3 \pm 0.7\%$  and the necrotic rate was  $21.2 \pm 4.6\%$  compared to  $0.4 \pm 0.2\%$  for apoptosis and  $0.4 \pm 0.4\%$  for necrosis in the control group. When the concentration of EPS increased to 1.0 mg/ml, the necrotic rate of cells was markedly increased from  $21.2 \pm 4.6$  to  $41.7 \pm 6.6\%$  ( $P < 0.05$ ). However, there was no significant difference regarding the apoptotic rate between treatment with EPS concentrations of 0.6 and 1.0 mg/ml ( $P > 0.05$ ).

To further verify the promotion effect of EPS on necrosis, LDH release assay was performed. There is a positive linear relationship between the level of LDH release and the necrotic rate. As shown in Fig. 2L, as the EPS concentration increased, the level of LDH release was significantly elevated in a concentration-dependent manner.

At the concentration of 1.0 mg/ml, the LDH release rate was  $0.455 \pm 0.021$  ( $P < 0.001$ ), which was consistent with the necrotic rate determined by Hoechst 33342/PI staining.

**Effects of EPS on the intracellular ROS level.** To investigate the oxidative damage effects of EPS on 786-O cells, ROS assay was performed to measure the intracellular ROS level.  $H_2DCFDA$  can be hydrolyzed by intracellular esterases, whereas ROS oxidates non-fluorescent  $H_2DCFDA$  to convert to the highly fluorescent 2',7'-dichlorofluorescein (DCF). Thus the level of green fluorescence can indicate the intracellular ROS level. As shown in Fig. 3, the intracellular ROS level was significantly elevated compared to that noted in the control group after EPS exposure ( $P < 0.01$ ). However, in the presence of 10 mM NAC, the level of intracellular ROS was significantly decreased compared to that following treatment with 0.6 mg/ml EPS alone ( $P < 0.05$ ). However, there was no obvious concentration-dependent trend in the EPS-induced ROS increase ( $P > 0.05$ ).

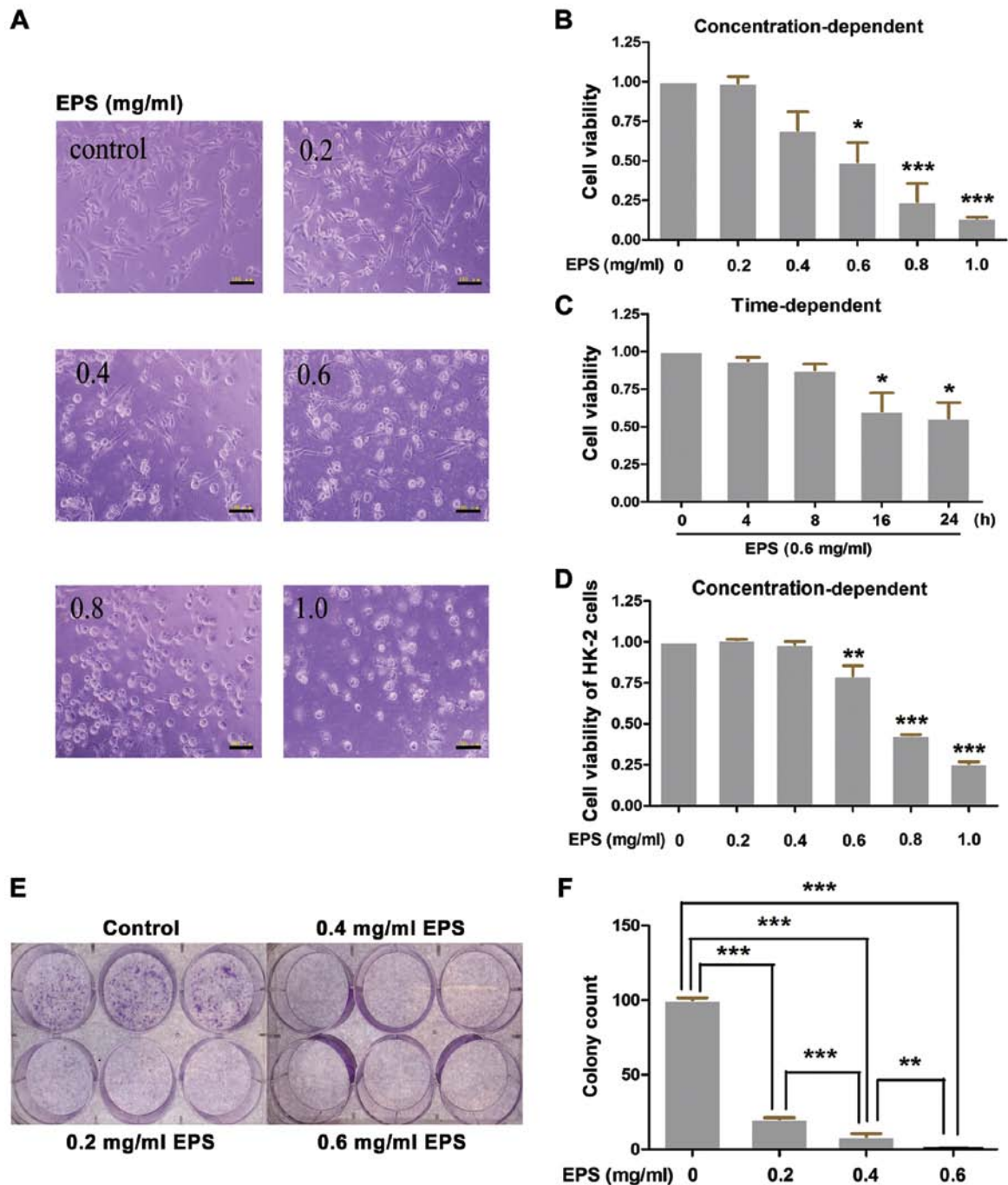


Figure 1. Ethanol extract of *Patrinia scabiosaefolia* (EPS) significantly inhibits the proliferation and growth of 786-O and HK-2 cells. (A and B) 786-O cells were cultured with different concentrations of EPS (0, 0.2, 0.4, 0.6, 0.8 and 1.0 mg/ml) for 24 h. (B) Then, cell viability was measured by MTT assay and (A) images of morphological alterations were captured by microscopy; \* $P < 0.05$ , \*\*\* $p < 0.001$ , vs. 0 mg/ml. (C) 786-O cells were incubated with EPS at 0.6 mg/ml, and then cell viability was measured at 0, 4, 8, 16 and 24 h, respectively; \* $P < 0.05$ , vs. 0 h. (D) HK-2 cells were cultured with different concentrations of EPS (0, 0.2, 0.4, 0.6, 0.8 and 1.0 mg/ml) for 24 h and then cell viability was measured by MTT assay; \*\* $P < 0.01$ , \*\*\* $p < 0.001$ , vs. 0 mg/ml. (E and F) Colony formation assay was performed. After incubation with different concentrations of EPS (0, 0.2, 0.4 and 0.6 mg/ml) for 24 h, 786-O cells were cultured for 10-14 days, and then the colony formation was determined. (E) The difference in the colony count was analyzed; \*\* $P < 0.01$ , \*\*\* $p < 0.001$ . All data were analyzed by one-way ANOVA with post hoc test ( $n=3$ ). Scale bars in A, 100  $\mu\text{m}$ .

**Effects of EPS on the intracellular calcium concentration.** To explore the metabolic perturbation effects of EPS on 786-O cells, we detected the intracellular calcium concentration by Fluo-3 AM probe. These probes specifically bind to  $[\text{Ca}^{2+}]_i$  and emit green fluorescence. As shown in Fig. 4, the mean fluorescence intensity of the EPS exposure group was significantly higher than that of the control group ( $P < 0.01$ ). In addition, the

above effects were significantly enhanced with the increase in EPS concentration ( $P < 0.001$ ).

**EPS downregulates the expression of SIRT-1 and induces the dephosphorylation of mTOR.** Western blotting was performed to investigate the involvement of SIRT-1 and mTOR signaling in the antitumor effects of EPS. As shown

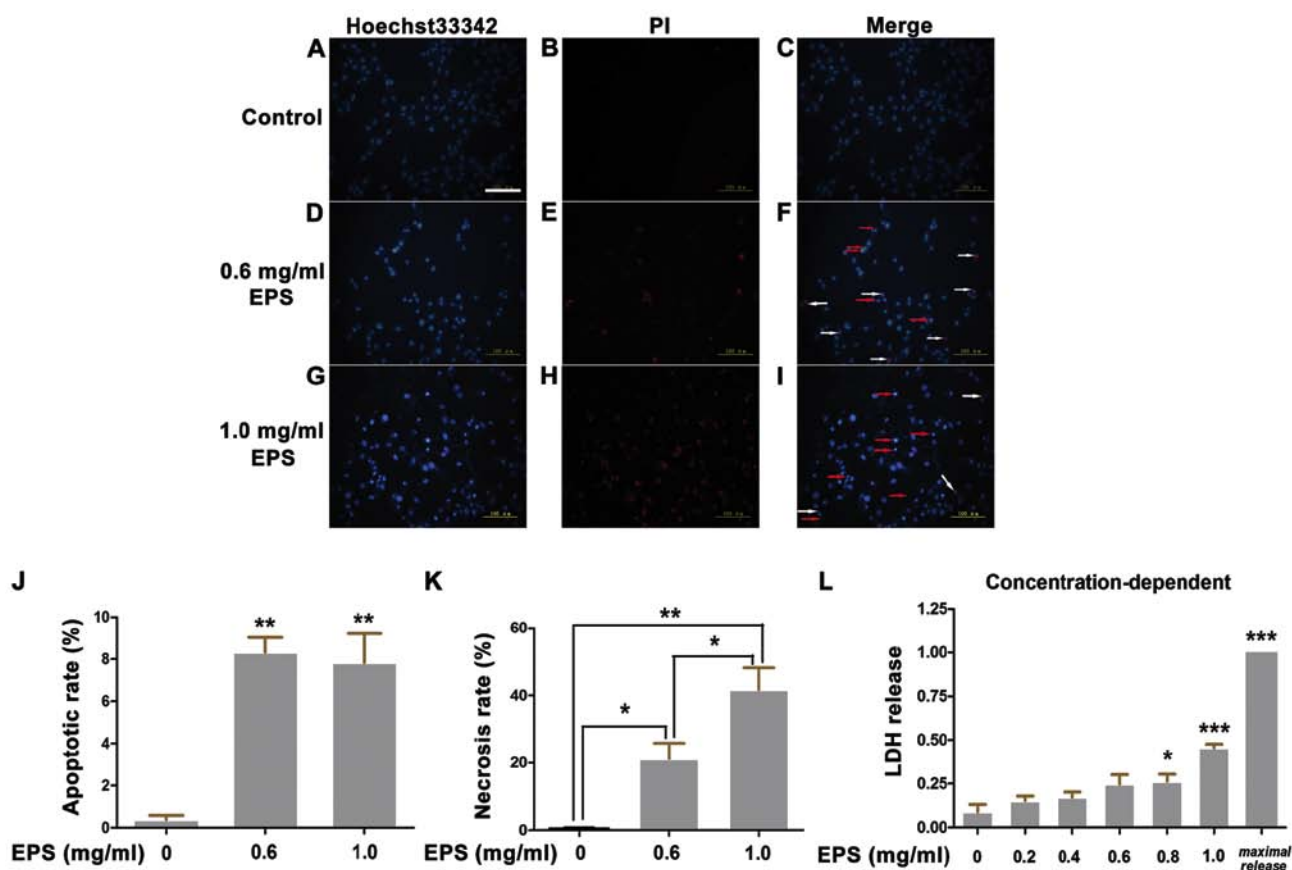


Figure 2. Ethanol extract of *Patrinia scabiosaefolia* (EPS) markedly promotes the apoptosis and necrosis of 786-O cells. 786-O cells were cultured with different concentrations of EPS (0, 0.6 and 1.0 mg/ml) for 24 h before Hoechst/PI staining and LDH release measurement. (A-I) Morphological changes were observed by fluorescence microscopy. Red fluorescence indicates necrotic cells whereas bright blue fluorescence indicates apoptotic cells. White arrows indicate necrotic cells whereas yellow arrows indicate apoptotic cells. (J) Apoptotic rate; \*\* $P < 0.01$ , vs. 0 mg/ml. (K) Necrosis rate; \* $P < 0.05$ , 0.6 mg/ml vs. 0 mg/ml and 1.0 vs. 0.6 mg/ml; \*\* $P < 0.01$ , 0 mg/ml vs. 1.0 mg/ml. (L) LDH release; \* $P < 0.05$ , vs. 0 mg/ml; \*\*\* $P < 0.01$ , vs. 0 mg/ml. All data were analyzed by one-way ANOVA with post hoc test (n=3). Scale bars: A-I, 100  $\mu$ m.

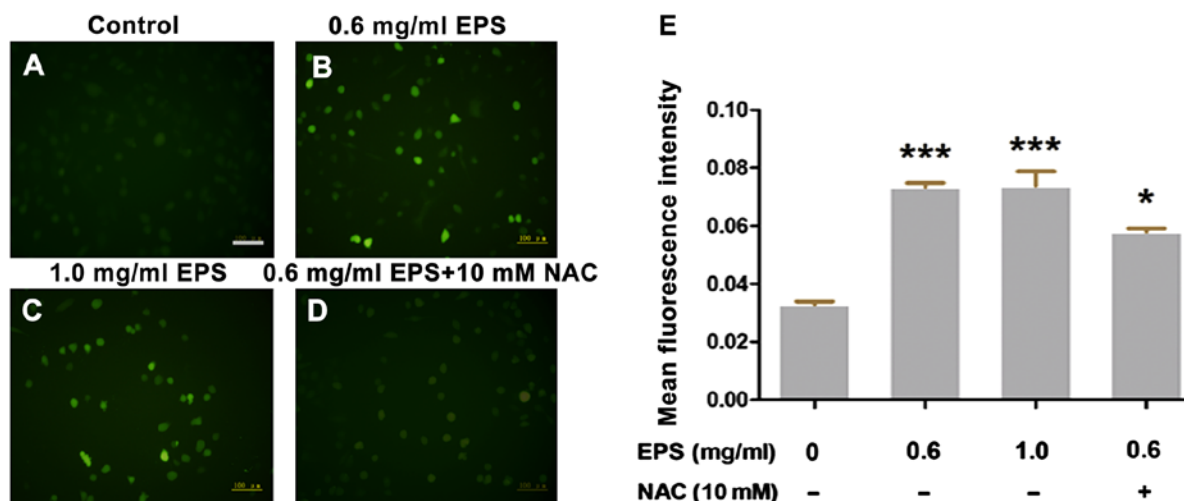


Figure 3. Ethanol extract of *Patrinia scabiosaefolia* (EPS) significantly induces intracellular ROS increase in 786-O cells. 786-O cells were incubated with different concentrations of EPS (0, 0.6 and 1.0 mg/ml) for 24 h (A-C) and with the presence of 10 mM NAC (D) before staining. The intensity of green fluorescence indicates the intracellular ROS level. (A-D) The morphological alterations were captured by fluorescence microscopy. (E) The mean fluorescent intensity was analyzed by ImageJ; \* $P < 0.05$ , vs. 0.6 mg/ml EPS only; \*\*\* $P < 0.001$ , vs. 0 mg/ml. All data were analyzed by one-way ANOVA with post hoc test (n=3). Scale bars: A-D, 100  $\mu$ m.

in Fig. 5, EPS significantly downregulated the expression of SIRT-1 ( $P < 0.05$ ) and decreased the ratio of p-mTOR/

mTOR ( $P < 0.001$ ) in the 786-O cells. Nevertheless, there was no statistically significant difference regarding the ratio of

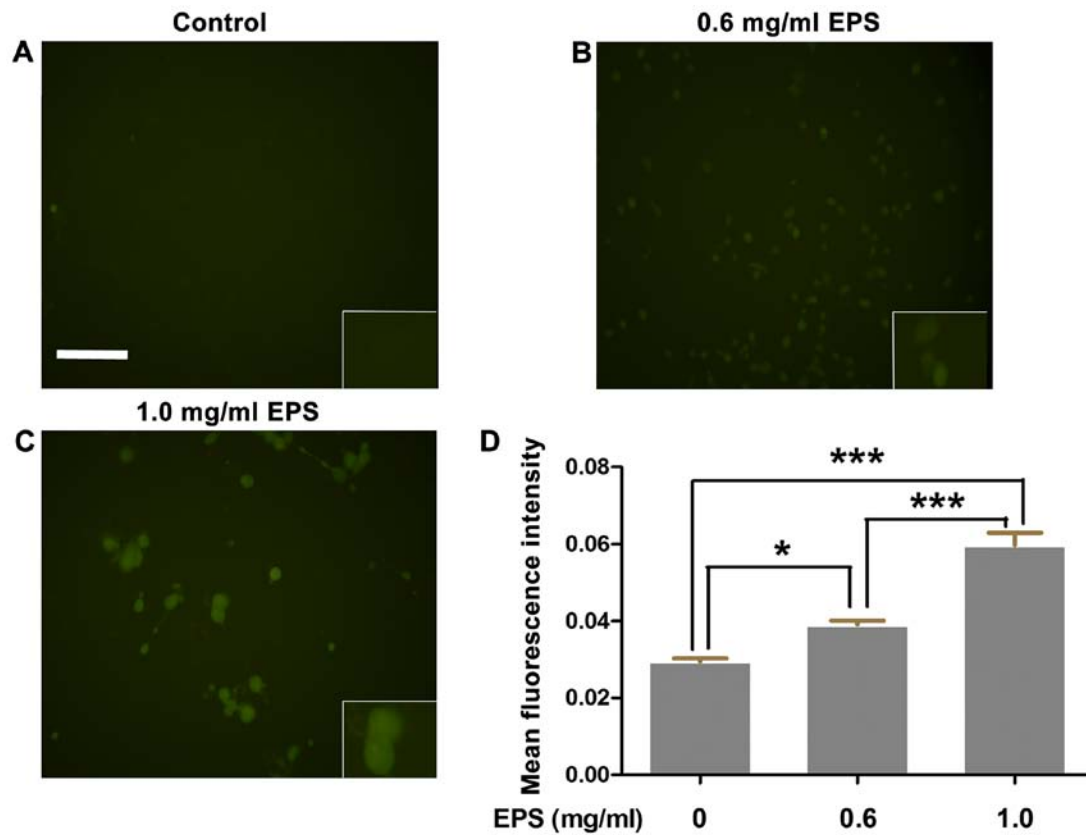


Figure 4. Effects of an ethanol extract of *Patrinia scabiosaefolia* (EPS) on intracellular calcium concentration. After incubation with different concentrations of EPS (0, 0.6 and 1.0 mg/ml), 786-O cells were stained for  $[Ca^{2+}]_i$ . The intensity of green fluorescence represents the intracellular calcium concentration. (A-C) The morphological alterations were captured by fluorescence microscopy. Scale bars: A-C, 100  $\mu$ m. (D) The mean fluorescent intensity was analyzed by ImageJ. All data were analyzed by one-way ANOVA with post hoc test (n=3); \*P<0.05, \*\*\*p<0.001.

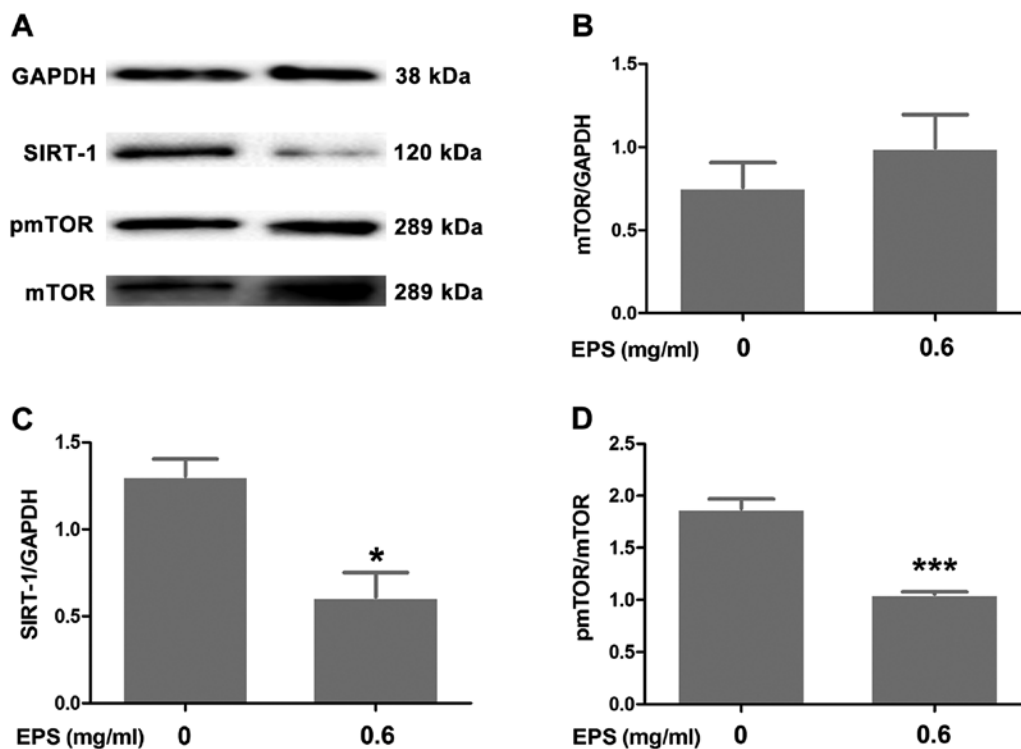


Figure 5. Ethanol extract of *Patrinia scabiosaefolia* (EPS) significantly suppresses the expression of SIRT-1 and induces the dephosphorylation of mTOR. 786-O cells were cultured with different concentrations of EPS (0 and 0.6 mg/ml) for 24 h and then the proteins were collected for western blotting. GAPDH was used as a loading control. (A) The representative bands of interest and (B-D) the statistical analyses of the gray scale are represented. SIRT-1 was normalized to GAPDH. Phosphorylated mTOR was normalized to total mTOR. Total mTOR was normalized to GAPDH; \*P<0.05, \*\*\*P<0.001, vs. 0 mg/ml. All data were analyzed by unpaired t-test (n=3).

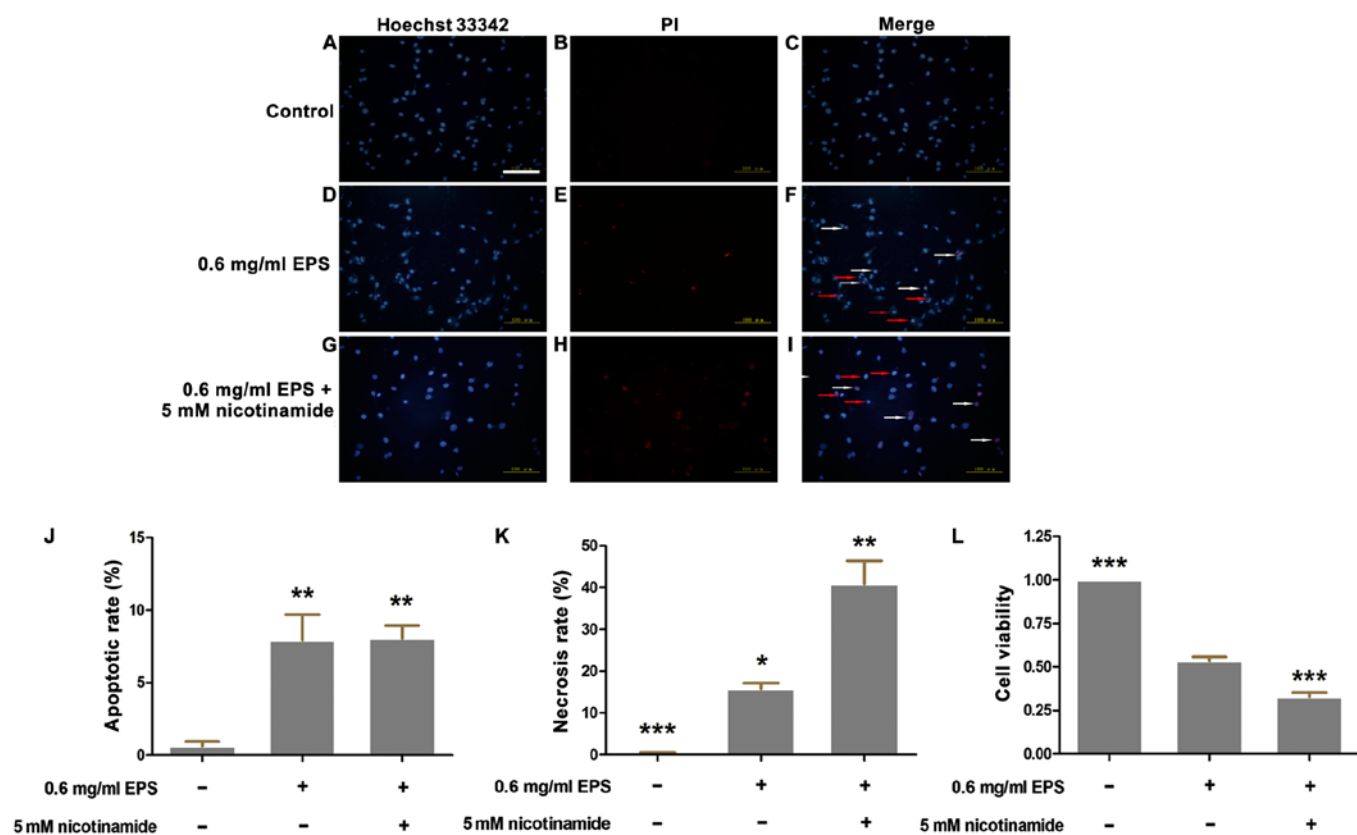


Figure 6. Nicotinamide partly enhances the antitumor effects of EPS. 786-O cells were incubated at different concentrations (0 and 0.6 mg/ml) of EPS with or without the presence of 5 mM nicotinamide for 24 h. (A-I) The morphological changes were observed by fluorescent microscopy. White arrows indicate necrotic cells whereas yellow arrows indicate apoptotic cells. Scale bars: A-I, 100  $\mu$ m. (J) Apoptotic rate as detected by Hoechst 33342/PI staining; \*\* $P < 0.01$  vs. 0 mg/ml. (K) Necrotic rate as detected by Hoechst 33342/PI staining; \* $P < 0.05$ , vs. 0 mg/ml; \*\* $P < 0.01$ , vs. 0.6 mg/ml EPS; \*\*\* $P < 0.001$  vs. 0.6 mg/ml EPS + 5 mM nicotinamide. (L) MTT assay was performed to measure the cell viability; \*\*\* $P < 0.001$  vs. 0.6 mg/ml EPS. All data were analyzed by one-way ANOVA with post hoc test ( $n=3$ ).

mTOR/GAPDH between the EPS exposure group and the control group ( $P > 0.05$ ).

*SIRT-1 inhibitor nicotinamide partly enhances the antitumor effects of EPS.* To further corroborate the involvement of SIRT-1 signaling in the antitumor effects of EPS, nicotinamide, a specific SIRT-1 inhibitor, was adopted for co-incubation with EPS. Cell viability assay and Hoechst 33342/PI double staining were carried out to explore the synergetic effects of nicotinamide. As shown in Fig. 6, the cells co-cultured with EPS plus nicotinamide had a significantly higher necrotic rate of  $40.9 \pm 5.5\%$  than that of  $15.8 \pm 1.3\%$  in the EPS group (without nicotinamide,  $P < 0.01$ ). The results of the MTT assay verified the above phenomena. The cell viability of the nicotinamide and EPS exposure group was significantly lower ( $0.33 \pm 0.02$ ) compared to the EPS exposure group ( $0.54 \pm 0.02$ ) ( $P < 0.001$ ). However, there was no significant difference regarding the apoptotic rate between the nicotinamide and EPS exposure group and the EPS exposure only group ( $P > 0.05$ ).

## Discussion

In the present study, we initially investigated the antitumor effects of EPS on 786-O cells *in vitro*. Our results demonstrated that EPS showed vigorous antiproliferation and growth inhibitory effects even at a low concentration of 0.6 mg/ml, which

needed a x500 dilution of the stock solution. Certain fluorescence staining assays were performed to identify the manner of cell death and the involvement of metabolic disruption. The results indicated that an increase in ROS and calcium overload may be responsible for the processes of metabolic perturbations. Furthermore, the underlying molecular mechanism was explored and we found that SIRT-1 and mTOR signaling were involved in the antitumor effects of EPS.

Previous studies have reported that *Patrinia scabiosaefolia* showed marked antiproliferation effects on various types of tumor cells, including HT-29, MCF-7 and HeLa cells (4,10,26). Our results demonstrated that EPS significantly decreased the cell viability of 786-O cells in concentration- and time-dependent manners. As shown in Fig. 1A, the effects of EPS on cells involved not only antiproliferation, but also death-promotion based on morphological observation. Moreover, EPS markedly impeded the formation of cell colonies. However, the concentration-dependent tendency in the colony formation assay was not in accordance with the MTT results. We speculated that the lower initial cell seeding number may be responsible for this inconsistency. The interactions of cells are vital to their survival. Thus, a lower cell number made the cells more vulnerable to EPS. As shown in Fig. 1D, EPS showed significant antiproliferation effects on HK-2 cells. However, at the concentration of 0.6 and 1.0 mg/ml, the cell viabilities of HK-2 cells were  $0.793 \pm 0.062$  and  $0.257 \pm 0.013$ , while cell

viabilities of 786-O were  $0.493 \pm 0.124$  and  $0.136 \pm 0.008$ . This result indicated that EPS exhibited, at least partly, specificity in regards to its antitumor effects.

Metabolic reprogramming, which refers to a series of metabolic alterations that stem from the molecular level, is a distinguishing characteristic of cancer cells (11). Changes in metabolism are critical for malignant proliferation and metastasis. However, these alterations also make the cells more susceptible to disruptions due to its metabolic dependency (27). As an essential role of metabolic regulation, ROS can affect the metabolism of cancer cells (12), and further cause cascaded reactions of metabolic perturbations including  $\text{Ca}^{2+}$  overload and apoptosis (14,16). Our results showed that EPS significantly induced apoptosis and necrosis of 786-O cells. However, intracellular  $\text{Ca}^{2+}$  and ROS levels were markedly elevated after the exposure of EPS, while the antioxidant NAC partly reversed the increase in ROS induced by EPS. Therefore, metabolic disruptions may mediate the antitumor effects of EPS, which indicate a new target for cancer intervention.

SIRT-1, as an  $\text{NAD}^+$ -dependent deacetylase, has been demonstrated to mediate extensive cellular metabolic processes including cell stress response, apoptosis and cell cycle arrest (17-19). SIRT-1 deacetylates a series of downstream molecules and induces extensive alterations, including an increase in ROS and apoptosis (28,29). Previous research has reported that MHY2256, an SIRT inhibitor, showed significant anticancer effects on MCF-7 and SKOV-3 cells through p53 acetylation (30). Accumulated evidence has demonstrated that overexpression of SIRT-1 is found in many malignant tumors including gastric cancer, hepatocellular carcinoma tissues, ovarian epithelial tumors and is closely linked with poor survival outcomes (21,31,32). Our results showed that the expression of SIRT-1 was significantly downregulated after EPS exposure, which was consistent with the above literature. Mammalian target of rapamycin (mTOR), formed by mTOR complex 1 (mTORC1) and mTOR complex 2 (mTORC2), has been implicated in metabolism, tumorigenesis and aging (24,33,34). The mTOR signaling pathway is involved in energy conservation, growth and division based on its protein kinase characteristics. PI3K/Akt/mTOR and mTOR/P53/P21 pathways have been demonstrated to be involved in antitumor effects by induction of autophagy and inhibition of proliferation (35,36). Wu *et al* reported that the Akt/GSK3 $\beta$ /mTOR pathway executes the effects of neuroprotection through an antioxidative mechanism (37). However, previous studies and clinical practice have also demonstrated that rapamycin, a specific inhibitor of mTOR, shows marked antitumor effects (24). Our results indicated that EPS obviously decreased the ratio of pmTOR/mTOR compared to the control group, which suggests that dephosphorylation of mTOR may induce the antitumor effects of EPS.

SIRT-1 and mTOR both mediate crucial molecular pathways in the signaling transduction network. However, there is no direct and explicit link between the two regulators to date (17). Previous study has reported that SIRT-1 negatively regulated mTOR signaling potentially mediated by sclerosis complex 2 (TSC2) (17). Guo *et al* reported that SIRT-1 mediated neuron regeneration by suppressing mTOR signaling (38). Nevertheless, there is evidence indicating that plumbagin induced the apoptosis and autophagy in prostate cancer cells by

inhibition of both SIRT-1 and mTOR signaling (39). Therefore, to further substantiate the involvement of SIRT-1 signaling, we employed nicotinamide, an inhibitor of SIRT-1, to block expression of SIRT-1 signaling. The results demonstrated that nicotinamide significantly enhanced the antitumor effects of EPS, which matched our original inference.

However, the role of SIRT-1 and mTOR regarding tumorigenesis is still controversial and there must be several intermediate molecules between SIRT-1 and mTOR. Zhang *et al* reported that the behaviors of SIRT-1 in tumorigenesis depend on p53 mutations (18). Thus, the alterations of P53 in cancer tissue, along with SIRT-1 and mTOR signaling, deserve much attention in future experiments. Otherwise, given to the involvement of intracellular ROS, the role of MAPKs needs to be further investigated. The MAPK cascade can be activated by ROS via various mechanisms (40). Thus, elucidation of MAPK alterations may provide new insight into the mechanism underlying the antitumor effects of EPS.

Based on previous literature, 10 bioactive agents have been identified (41), including iridoids (42), saponins (41,43), triterpenes (44,45) and lactones (46). Detailed chemical fingerprint of NMR can be reviewed in the above literature. Forty-four essential oils of *Patrinia scabiosaeifolia* have been identified by chemical fingerprinting of GC (Gas Chromatography) (4). Thus, identification of these bioactive components can provide valuable directions for further research.

In summary, the present study investigated the effects of EPS on 786-O cells and partly validated the involvement of ROS and  $\text{Ca}^{2+}$ -mediated SIRT-1 and mTOR signaling. We highlighted the markedly antitumor effects of EPS and provide novel insight in drug discovery for cancer treatments.

## Acknowledgements

The present study was supported by grants of the National Natural Science Foundation of China (nos. 81372335, 81400696 and 81502213), a grant of the Shandong Provincial Natural Science Foundation (ZR2014HQ026), a grant of the Bureau of Science and Technology of Jinan (no. 201303040), and the Science and Technology Development Project of Shandong (no. 2011GSF11807).

## References

1. Kan XX, Li Q, Chen X, Wang YJ, Li YJ, Yang Q, Xiao HB, Wang ZX, Chen Y, Weng XG, *et al*: A novel cell cycle blocker extracted from *Stellera chamaejasme* L. inhibits the proliferation of hepatocarcinoma cells. *Oncol Rep* 35: 3480-3488, 2016.
2. Gordaliza M: Natural products as leads to anticancer drugs. *Clin Transl Oncol* 9: 767-776, 2007.
3. Brglez Mojzer E, Knez Hrnčič M, Škerget M, Knez Ž and Bren U: Polyphenols: Extraction methods, antioxidative action, bioavailability and anticarcinogenic effects. *Molecules* 21: 21, 2016.
4. Lin J, Cai QY, Xu W, Lin JM and Peng J: Chemical composition, anticancer, anti-neuroinflammatory, and antioxidant activities of the essential oil of *Patrinia scabiosaeifolia*. *Chin J Integr Med*: Sep 1, 2016 (Epub ahead of print).
5. Cho EJ, Shin JS, Noh YS, Cho YW, Hong SJ, Park JH, Lee JY, Lee JY and Lee KT: Anti-inflammatory effects of methanol extract of *Patrinia scabiosaeifolia* in mice with ulcerative colitis. *J Ethnopharmacol* 136: 428-435, 2011.
6. Zhang M, Sun G, Shen A, Liu L, Ding J and Peng J: *Patrinia scabiosaeifolia* inhibits the proliferation of colorectal cancer *in vitro* and *in vivo* via  $\text{G}_1/\text{S}$  cell cycle arrest. *Oncol Rep* 33: 856-860, 2015.



7. Ju HK, Baek SH, An RB, Bae K, Son KH, Kim HP, Kang SS, Lee SH, Son JK and Chang HW: Inhibitory effects of nardostachin on nitric oxide, prostaglandin E<sub>2</sub>, and tumor necrosis factor- $\alpha$  production in lipopolysaccharide activated macrophages. *Biol Pharm Bull* 26: 1375-1378, 2003.
8. Chen L, Liu L, Ye L, Shen A, Chen Y, Sferra TJ and Peng J: *Patrinia scabiosaefolia* inhibits colorectal cancer growth through suppression of tumor angiogenesis. *Oncol Rep* 30: 1439-1443, 2013.
9. Peng J, Chen Y, Lin J, Zhuang Q, Xu W, Hong Z and Sferra TJ: *Patrinia scabiosaefolia* extract suppresses proliferation and promotes apoptosis by inhibiting the STAT3 pathway in human multiple myeloma cells. *Mol Med Rep* 4: 313-318, 2011.
10. Chiu LC, Ho TS, Wong EY and Ooi VE: Ethyl acetate extract of *Patrinia scabiosaefolia* downregulates anti-apoptotic Bcl-2/Bcl-X<sub>L</sub> expression, and induces apoptosis in human breast carcinoma MCF-7 cells independent of caspase-9 activation. *J Ethnopharmacol* 105: 263-268, 2006.
11. Schulze A and Harris AL: How cancer metabolism is tuned for proliferation and vulnerable to disruption. *Nature* 491: 364-373, 2012.
12. Trachootham D, Alexandre J and Huang P: Targeting cancer cells by ROS-mediated mechanisms: A radical therapeutic approach? *Nat Rev Drug Discov* 8: 579-591, 2009.
13. Panieri E and Santoro MM: ROS homeostasis and metabolism: A dangerous liason in cancer cells. *Cell Death Dis* 7: e2253, 2016.
14. Yan Y, Wei CL, Zhang WR, Cheng HP and Liu J: Cross-talk between calcium and reactive oxygen species signaling. *Acta Pharmacol Sin* 27: 821-826, 2006.
15. Ganie SA, Dar TA, Bhat AH, Dar KB, Anees S, Zargar MA and Masood A: Melatonin: A potential anti-oxidant therapeutic agent for mitochondrial dysfunctions and related disorders. *Rejuvenation Res* 19: 21-40, 2016.
16. Li Z, Wang H, Wang Q and Sun J: Buyang Huanwu decoction vigorously rescues PC12 cells against 6-OHDA-induced neurotoxicity via Akt/GSK3 $\beta$  pathway based on serum pharmacology methodology. *Rejuvenation Res* 19: 467-477, 2016.
17. Ghosh HS, McBurney M and Robbins PD: SIRT1 negatively regulates the mammalian target of rapamycin. *PLoS One* 5: e9199, 2010.
18. Zhang ZY, Hong D, Nam SH, Kim JM, Paik YH, Joh JW, Kwon CH, Park JB, Choi GS, Jang KY, *et al*: SIRT1 regulates oncogenesis via a mutant p53-dependent pathway in hepatocellular carcinoma. *J Hepatol* 32: 121-130, 2015.
19. Liu Z, Gu H, Gan L, Xu Y, Feng F, Saeed M and Sun C: Reducing Smad3/ATF4 was essential for Sirt1 inhibiting ER stress-induced apoptosis in mice brown adipose tissue. *Oncotarget* 8: 9267-9279, 2017.
20. Jang KY, Hwang SH, Kwon KS, Kim KR, Choi HN, Lee NR, Kwak JY, Park BH, Park HS, Chung MJ, *et al*: SIRT1 expression is associated with poor prognosis of diffuse large B-cell lymphoma. *Am J Surg Pathol* 32: 1523-1531, 2008.
21. Chen HC, Jeng YM, Yuan RH, Hsu HC and Chen YL: SIRT1 promotes tumorigenesis and resistance to chemotherapy in hepatocellular carcinoma and its expression predicts poor prognosis. *Ann Surg Oncol* 19: 2011-2019, 2012.
22. Lee H, Kim KR, Noh SJ, Park HS, Kwon KS, Park BH, Jung SH, Youn HJ, Lee BK, Chung MJ, *et al*: Expression of DBC1 and SIRT1 is associated with poor prognosis for breast carcinoma. *Hum Pathol* 42: 204-213, 2011.
23. Dibble CC and Cantley LC: Regulation of mTORC1 by PI3K signaling. *Trends Cell Biol* 25: 545-555, 2015.
24. Zoncu R, Efeyan A and Sabatini DM: mTOR: From growth signal integration to cancer, diabetes and ageing. *Nat Rev Mol Cell Biol* 12: 21-35, 2011.
25. Menendez JA and Lupu R: Fatty acid synthase and the lipogenic phenotype in cancer pathogenesis. *Nat Rev Cancer* 7: 763-777, 2007.
26. Liu L, Shen A, Chen Y, Wei L, Lin J, Sferra TJ, Hong Z and Peng J: *Patrinia scabiosaefolia* induces mitochondrial-dependent apoptosis in a mouse model of colorectal cancer. *Oncol Rep* 30: 897-903, 2013.
27. Cairns RA, Harris IS and Mak TW: Regulation of cancer cell metabolism. *Nat Rev Cancer* 11: 85-95, 2011.
28. Liu X, Yang T, Sun T and Shao K: SIRT1 mediated regulation of oxidative stress induced by *Pseudomonas aeruginosa* lipopolysaccharides in human alveolar epithelial cells. *Mol Med Rep* 15: 813-818, 2017.
29. Li B, He X, Zhuang M, Niu B, Wu C, Mu H, Tang F, Cui Y, Liu W, Zhao B, *et al*: Melatonin ameliorates busulfan-induced spermatogonial stem cell oxidative apoptosis in mouse testes. *Antioxid Redox Signal*: Jan. 27, 2017 (Epub ahead of print). doi: 10.1089/ars.2016.6792.
30. Park EY, Woo Y, Kim SJ, Kim DH, Lee EK, De U, Kim KS, Lee J, Jung JH, Ha KT, *et al*: Anticancer effects of a new SIRT inhibitor, MHY2256, against human breast cancer MCF-7 cells via regulation of MDM2-p53 binding. *Int J Biol Sci* 12: 1555-1567, 2016.
31. Zhang S, Huang S, Deng C, Cao Y, Yang J, Chen G, Zhang B, Duan C, Shi J, Kong B, *et al*: Co-ordinated overexpression of SIRT1 and STAT3 is associated with poor survival outcome in gastric cancer patients. *Oncotarget* 8: 18848-18860, 2017.
32. Jang KY, Kim KS, Hwang SH, Kwon KS, Kim KR, Park HS, Park BH, Chung MJ, Kang MJ, Lee DG, *et al*: Expression and prognostic significance of SIRT1 in ovarian epithelial tumours. *Pathology* 41: 366-371, 2009.
33. Kim I, Rodriguez-Enriquez S and Lemasters JJ: Selective degradation of mitochondria by mitophagy. *Arch Biochem Biophys* 462: 245-253, 2007.
34. Brachmann SM, Hofmann I, Schnell C, Fritsch C, Wee S, Lane H, Wang S, Garcia-Echeverria C and Maira SM: Specific apoptosis induction by the dual PI3K/mTOR inhibitor NVP-BE225 in HER2 amplified and PIK3CA mutant breast cancer cells. *Proc Natl Acad Sci USA* 106: 22299-22304, 2009.
35. Chen J, Yuan J, Zhou L, Zhu M, Shi Z, Song J, Xu Q, Yin G, Lv Y, Luo Y, *et al*: Regulation of different components from *Ophiopogon japonicus* on autophagy in human lung adenocarcinoma A549 cells through PI3K/Akt/mTOR signaling pathway. *Biomed Pharmacother* 87: 118-126, 2017.
36. Lin F, Lei S, Ma J, *et al*: [Inhibitory effect of jianpi-jiedu prescription-contained serum on colorectal cancer SW48 cell proliferation by mTOR-P53-P21 signalling pathway]. *Zhong Nan Da Xue Xue Bao Yi Xue Ban* 41: 1128-1136, 2016 (abstract in English).
37. Wu J, Zhu D, Zhang J, Li G, Liu Z and Sun J: Lithium protects against methamphetamine-induced neurotoxicity in PC12 cells via Akt/GSK3 $\beta$ /mTOR pathway. *Biochem Biophys Res Commun* 465: 368-373, 2015.
38. Guo W, Qian L, Zhang J, Zhang W, Morrison A, Hayes P, Wilson S, Chen T and Zhao J: Sirt1 overexpression in neurons promotes neurite outgrowth and cell survival through inhibition of the mTOR signaling. *J Neurosci Res* 89: 1723-1736, 2011.
39. Zhou ZW, Li XX, He ZX, Pan ST, Yang Y, Zhang X, Chow K, Yang T, Qiu JX, Zhou Q, *et al*: Induction of apoptosis and autophagy via sirtuin1- and PI3K/Akt/mTOR-mediated pathways by plumbagin in human prostate cancer cells. *Drug Des Devel Ther* 9: 1511-1554, 2015.
40. Son Y, Cheong YK, Kim NH, Chung HT, Kang DG and Pae HO: Mitogen-activated protein kinases and reactive oxygen species: How can ROS activate MAPK pathways? *J Signal Transduct* 2011: 792639, 2011.
41. Gao L, Zhang L, Li N, Liu JY, Cai PL and Yang SL: New triterpenoid saponins from *Patrinia scabiosaefolia*. *Carbohydr Res* 346: 2881-2885, 2011.
42. Taguchi H and Endo T: Letter: Patrinoside, a new iridoid glycoside from *Patrinia scabiosaefolia*. *Chem Pharm Bull* 22: 1935-1937, 1974.
43. Nakanishi T, Tanaka K, Murata H, Somekawa M and Inada A: Phytochemical studies of seeds of medicinal plants. III. Ursolic acid and oleanolic acid glycosides from seeds of *Patrinia scabiosaefolia* Fischer. *Chem Pharm Bull* 41: 183-186, 1993.
44. Choi JS and Woo WS: Triterpenoid glycosides from the roots of *Patrinia scabiosaefolia*. *Planta Med* 53: 62-65, 1987.
45. Inada A, Yamada M, Murata H, Kobayashi M, Toya H, Kato Y and Nakanishi T: Phytochemical studies of seeds of medicinal plants. I. Two sulfated triterpenoid glycosides, sulfapatrinosides I and II, from seeds of *Patrinia scabiosaefolia* FISCHER. *Chem Pharm Bull* 36: 4269-4274, 1988.
46. Yang MY, Choi YH, Yeo H and Kim J: A new triterpene lactone from the roots of *Patrinia scabiosaefolia*. *Arch Pharm Res* 24: 416-417, 2001.